

## **THERMOELECTRIC PROPERTIES OF Ru<sub>2</sub>Si<sub>3</sub> PREPARED BY SPARK PLASMA SINTERING METHOD**

*Y. Arita<sup>1\*</sup>, S. Mitsuda<sup>2</sup> and T. Matsui<sup>2</sup>*

<sup>1</sup>Research Center for Nuclear Materials Recycle, Nagoya University, Furo-cho, Chikusa-ku, Nagoya 464-8603, Japan

<sup>2</sup>Department of Quantum Engineering, Graduate School of Engineering, Nagoya University, Furo-cho, Chikusa-ku, Nagoya 464-8603, Japan

### **Abstract**

Electrical conductivities, Seebeck coefficients and thermal diffusivities were measured for Ru<sub>2</sub>Si<sub>3</sub> samples with different densities prepared by spark plasma sintering method and an Rh-doped sample prepared by the floating zone melting and spark plasma sintering methods. Electrical conductivities, Seebeck coefficients and thermal diffusivities increased with sample density for undoped Ru<sub>2</sub>Si<sub>3</sub>. The thermoelectrical figure of merit also increased with sample density. Electrical conductivity of the 4% Rh-doped sample was larger than that of our previous samples prepared by floating zone melting method. Values of Seebeck coefficients were similar for samples prepared by either method.

**Keywords:** electrical conductivity, Ru<sub>2</sub>Si<sub>3</sub>, Seebeck coefficient, thermal diffusivity, thermoelectric material

### **Introduction**

To solve global environmental and energy problems, solid state direct energy conversion has been regarded as promising. Although most commonly used thermoelectric materials, such as Bi<sub>2</sub>Te<sub>3</sub>, PbTe, and SiGe, show high thermoelectrical figures of merit  $ZT$ , values of  $ZT$  of these materials did not exceed unity; thus, their thermoelectrical efficiencies remain relatively low. The dimensionless thermoelectric figure of merit  $ZT$  is given as

$$ZT = \alpha^2 \sigma T / \lambda \quad (1)$$

where  $\sigma$  is the electrical conductivity,  $\alpha$  is the Seebeck coefficient,  $T$  is the absolute temperature, and  $\lambda$  is the thermal conductivity. In order to achieve significantly higher efficiencies (high  $ZT$ ), new materials are needed.

Ruthenium sesquisilicide (Ru<sub>2</sub>Si<sub>3</sub>) is an isostructural Nowotny chimney-ladder compound with valence electrons per metal atom (VEC)=14 [1]. An interesting char-

\* Author for correspondence: E-mail: y-arita@nucl.nagoya-u.ac.jp

acteristic of Nowotny chimney-ladder compounds is the magic number of 14 VEC, a remarkably predictive rule for occurrence of a band gap in these materials [2]. Fourteen valence electrons are enough to fill the 4 *s-p* type bonding states of this structure. A model for thermoelectric properties of doped Ru<sub>2</sub>Si<sub>3</sub> has been developed based on high-temperature data on electrical resistivity, the Hall effect, the Seebeck coefficient, and thermal conductivity in the intrinsic region of Ru<sub>2</sub>Si<sub>3</sub> [3]. From this model,  $ZT_{\max}$  for *p*-type Ru<sub>2</sub>Si<sub>3</sub> has been predicted to be three times larger than *p*-type SiGe; and that for *n*-type Ru<sub>2</sub>Si<sub>3</sub> was predicted to be 50% larger than *n*-type SiGe [4]. Although various preparation methods and many dopants have been investigated experimentally in order to obtain a much higher figure of merit for Ru<sub>2</sub>Si<sub>3</sub>, expected values of thermoelectricity have not been attained [5–9] due either to precipitations in single crystals produced from the reaction with the crucible used in Bridgman-like preparation methods, or to interruption in current paths at grain boundaries in polycrystalline samples. In our preceding study [10, 11], undoped Ru<sub>2</sub>Si<sub>3</sub> prepared by floating zone melting (FZ) method showed higher electrical conductivity than that of the single crystalline sample prepared by the Bridgman (BM) method. However, although FZ method is good for preparing highly efficient samples, sample shape is limited to small cylindrical ones.

This study used the spark plasma sintering (SPS) method to prepare samples with desired shapes. The dimensionless thermoelectric figure of merit (*ZT*) was calculated from measured Seebeck coefficients, electrical conductivities and thermal diffusivities for several samples with different densities.

## Experimental

### *Sample preparation*

Samples of undoped Ru<sub>2</sub>Si<sub>3</sub> were first made by arc melting cold-pressed pellets made of 99.9% pure ruthenium powder and a 99.999% pure silicon powder mixture under purified argon gas with a Ti getter. Then, the ingot sample was pulverized to powder that was again sintered by SPS method. In SPS method, the sample powder was filled into a graphite die and graphite punches were settled. Sintering was done by loading the pulse current (about 1000 A) in an argon atmosphere at high temperature for 20 min under pressure of about 45 MPa. Three sintering temperatures were selected to prepare samples with different densities. Sintering temperature and sample density (%TD: relative ratio to theoretical density) are listed in Table 1. Samples were blades of 1.5–2.5 mm thickness, 3 mm width and 20 mm length for electrical conductivity and Seebeck coefficient measurements; disks of 1.0–2.0 mm thickness and 10 mm diameter were used for thermal diffusivity measurement. A Ru<sub>2</sub>Si<sub>3</sub> sample doped with 4% Rh was made by arc melting first. Then a polycrystalline rod sample, prepared by the arc melting method, was recrystallized using the FZ method to eliminate impurities [10, 11]; this was done in a purified argon gas flow for preventing sample oxidation. The FZ method apparatus has two infrared heating furnaces of the double ellipsoidal type with two 1.5 kW halogen lamps as the heat source. Mass loss during

recrystallization was measured and found in all cases to be less than 1%. Next, FZ samples were crushed into powder and sintered by SPS at 1673 K. X-ray diffraction analysis indicated presence of a single phase for each sample.

*Measurements of thermoelectric properties* Table 1 Sintering conditions and sample densities

The Seebeck coefficient and electrical conductivity were measured simultaneously at each temperature. Electrical conductivity was measured by dc 4-probe technique using Pt wires of each thermocouple as current leads. Current was applied by a regulated dc power supply; voltage and current were measured with digital voltmeters. Seebeck coefficients were calculated from least squares regressions of thermoelectromotive forces as a function of temperature difference. Thermal diffusivities were measured using a laser flash method over the temperature range from 290 to 1170 K. Thermal diffusivity measurements of each specimen were carried out three times at each temperature in a vacuum of less than  $1 \cdot 10^{-2}$  Pa. Thermal diffusivities were estimated from time dependence of temperature for the rear sample surface using the curve fitting method [12].

**Table 1** Sintering conditions and sample densities

Sample	Sintering temperature/K	Density/%TD
1	1273	71
2	1473	86
3	1673	99

## Results and discussion

### *Undoped Ru<sub>2</sub>Si<sub>3</sub>*

Temperature dependencies of electrical conductivities of undoped Ru<sub>2</sub>Si<sub>3</sub> obtained in this study are shown in Fig. 1 in comparison with those prepared by the arc melted [4], the hot press [7], the Bridgman method [8], and FZ [10]. Electrical conductivity is seen to increase with increasing sample density. Temperature dependencies of Seebeck coefficients of undoped Ru<sub>2</sub>Si<sub>3</sub> are shown in Fig. 2 and exhibit *n*-type semiconducting behavior below about 750 K and *p*-type semiconducting behavior above 750 K. Seebeck coefficients are found to increase with sample density above 800 K. Thermal conductivity  $\kappa$  is given by Eq. (2) with heat capacity  $C_p$ , density  $\rho$  and thermal diffusivity  $\alpha$ .

$$\kappa = C_p \alpha \rho \quad (2)$$

In this study, the heat capacity value obtained by Kuntz [13] was used to calculate thermal conductivity. Thermal conductivities are shown in Fig. 3. Thermal

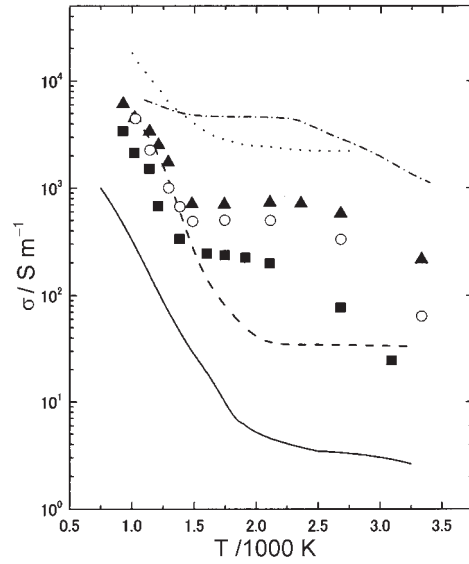


**Fig. 1** Electrical conductivity of undoped Ru<sub>2</sub>Si<sub>3</sub>; present data ( $\blacktriangle$  – 99%TD,  $\circ$  – 86%TD,  $\blacksquare$  – 71%TD), -.-.- hot press [7], — arc [4], ---- Bridgman [8], .... FZ [10]

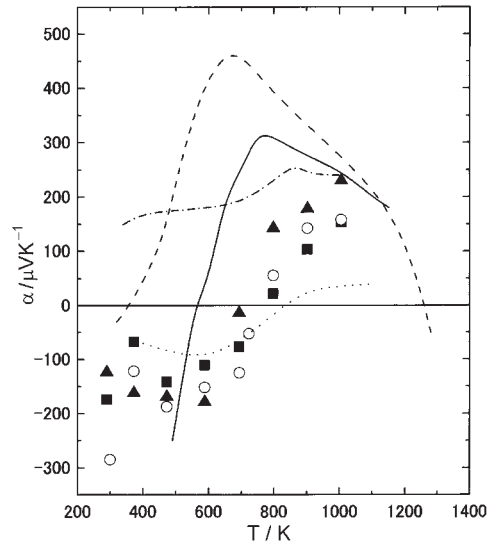


**Fig. 2** Seebeck coefficient of undoped Ru<sub>2</sub>Si<sub>3</sub>; present data ( $\blacktriangle$  – 99%TD,  $\circ$  – 86%TD,  $\blacksquare$  – 71%TD), -.-.- hot press [7], — arc [4], ---- Bridgman [8], .... FZ [10]

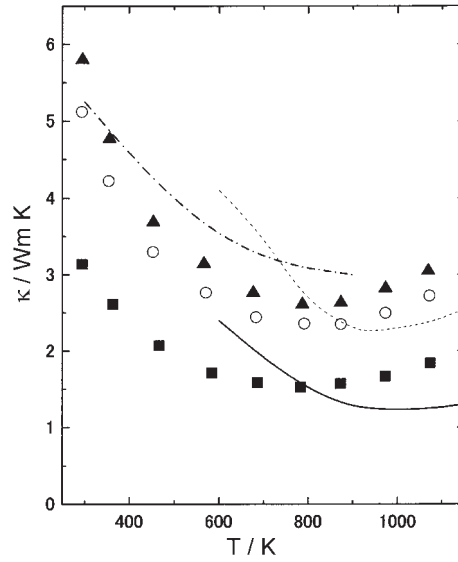


**Fig. 3** Thermal conductivity of undoped Ru<sub>2</sub>Si<sub>3</sub>; present data (▲ – 99%TD, ○ – 86%TD, ■ – 71%TD), - - - hot press [7], — arc [4], - · - · Bridgman [8], ··· FZ [10]

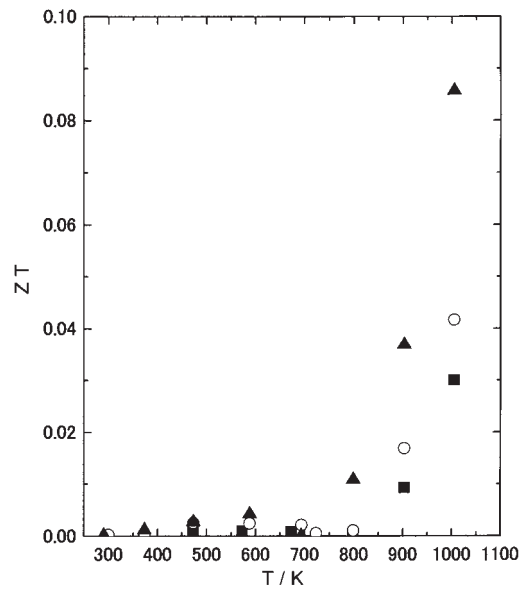


**Fig. 4** Dimensionless figure of merit of undoped Ru<sub>2</sub>Si<sub>3</sub>; ▲ – 99%TD, ○ – 86%TD, ■ – 71%TD

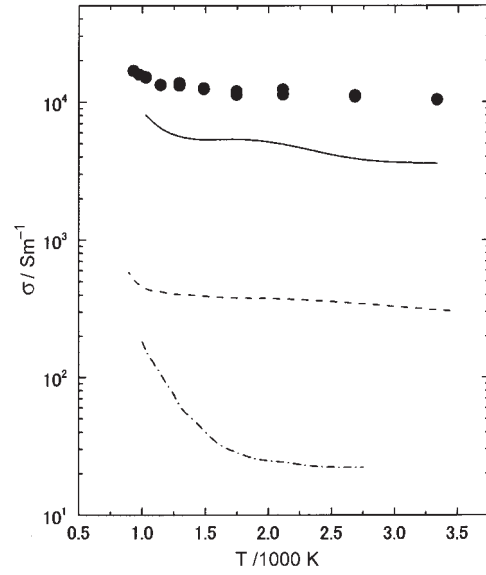


**Fig. 5** Electrical conductivity of 4% Rh-doped Ru<sub>2</sub>Si<sub>3</sub>; ● – this study, — FZ [11], ----- arc [10], -.-.- undoped FZ [10]

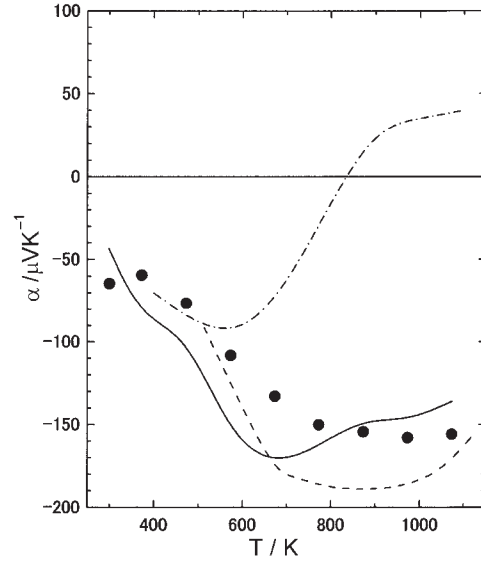


**Fig. 6** Seebeck coefficient of 4% Rh-doped Ru<sub>2</sub>Si<sub>3</sub>; ● – this study, — FZ [11], ----- arc [10], -.-.- undoped FZ [10]

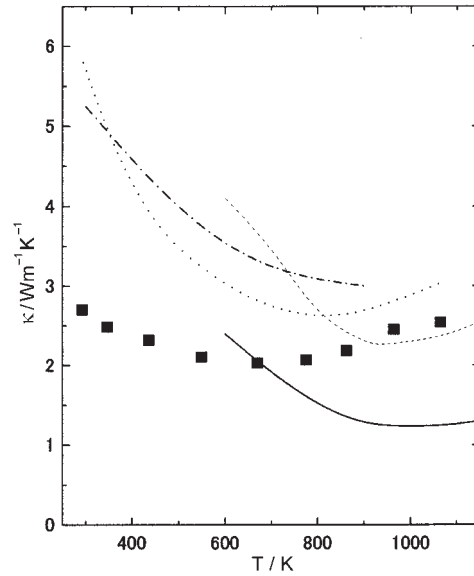


**Fig. 7** Thermal conductivity of 4% Rh-doped Ru<sub>2</sub>Si<sub>3</sub>; ■ – this study, ---- undoped hot press [7], — undoped arc [4], ---- undoped Bridgman [8], ···· undoped FZ+SPS (this study)

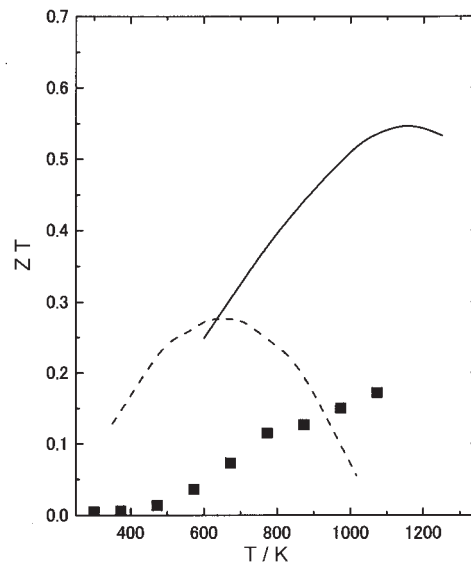


**Fig. 8** Dimensionless figure of merit of 4% Rh-doped Ru<sub>2</sub>Si<sub>3</sub>; ■ – this study, — optimized *n*-type SiGe [14], ---- FeSi<sub>2</sub> [15]

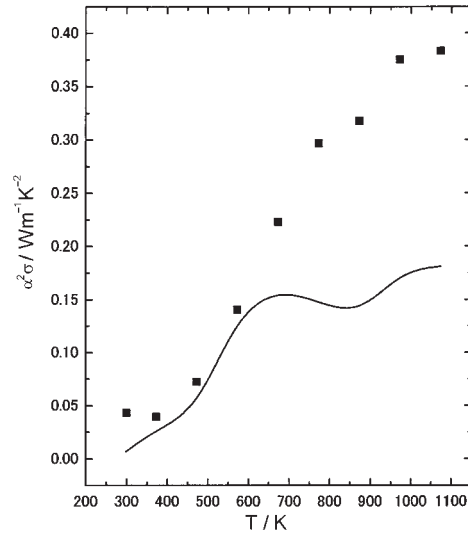


**Fig. 9** Power factor ( $\alpha^2\sigma$ ) of 4% Rh-doped Ru<sub>2</sub>Si<sub>3</sub>; ■ – this study, — FZ [11]

conductivity increases with increasing sample density. Thermal conductivity can be normalized using the density correlation factor  $\beta$  and Eq. (3)

$$\kappa_A = \kappa_B (1 - \beta(\rho_B - \rho_A) / \rho_B) \quad (3)$$

where subscript A and B represent each sample with different density. Values of  $\beta$  are in the range between 0.87 and 2.37. The  $ZT$  was then calculated from electric conductivity, Seebeck coefficient and thermal conductivity using Eq. (1) and is shown in Fig. 4. It is shown that the highly dense sample has high  $ZT$ . Density dependence of electrical conductivity canceled out the contribution of thermal conductivity with density for  $ZT$  value. As a result, the  $ZT$  value was mainly reflected by the Seebeck coefficient. Therefore, sintering temperature was decided to be 1673 K to make samples with high density.

#### *Rh-doped Ru<sub>2</sub>Si<sub>3</sub>*

Temperature dependencies of electrical conductivities and Seebeck coefficients are shown in Figs 5 and 6, respectively. Electrical conductivity of 4% Rh-doped Ru<sub>2</sub>Si<sub>3</sub> obtained in this study is shown in comparison with those prepared by arc melting [10], FZ only [11], and undoped FZ [10]. At room temperature, electrical conductivity of the FZ and SPS undoped sample decreased extremely by about two orders of magnitude compared to those of a typical arc sample [10], and one order of magnitude compared to that of undoped Ru<sub>2</sub>Si<sub>3</sub> by FZ method [11]. By doping with Rh, electrical conductivity of Ru<sub>2</sub>Si<sub>3</sub> was enhanced by about one order of magnitude in the extrinsic region. Seebeck coefficients of 4% Rh-doped Ru<sub>2</sub>Si<sub>3</sub> prepared by FZ and



SPS method were negative and reached a minimum around 700 K. Values of 4% Rh-doped samples made by FZ and SPS method in this study were not so different from those prepared by arc melting and FZ only [10].

Thermal conductivity was calculated using Eq. (2) and is shown in Fig. 7 with other experimental values. Rh-doping decreases thermal conductivity in comparison to that of an undoped SPS sample. Above 670 K, thermal conductivity increases with temperature. It is thought that the contribution of thermally activated charge carriers becomes large at high temperatures.

The dimensionless thermoelectric figure of merit ( $ZT$ ) values were then calculated using Eq. (1) and are shown in Fig. 8. The  $ZT$  characteristics are highly affected by electrical conductivity temperature dependence. The higher the temperature, the higher  $ZT$  becomes. At 1073 K,  $ZT$  was 0.172, the maximum performance in present data. The maximum  $ZT$  value of  $n$ -type Ru<sub>2</sub>Si<sub>3</sub> doped with 4% Rh seems to be about one-third that of optimized  $n$ -type Si-Ge [14]. The maximum  $ZT$  value is also two thirds of that for traditional thermoelectric material, FeSi<sub>2</sub>; however, it becomes larger than that of FeSi<sub>2</sub> above 950 K.

The power factor ( $\alpha^2\sigma$ ) is shown in Fig. 9 for comparison of effects of each sample fabrication method. The power factor of the FZ+SPS sample is larger than that of the FZ sample above 700 K and about twice as high as at 1073 K. It is thought that the SPS process can reduce electrical resistance similarly to a microcrack in the specimen compared with the FZ.

## Conclusions

Thermoelectric properties were measured for undoped Ru<sub>2</sub>Si<sub>3</sub> samples prepared by spark plasma sintering (SPS) method and 4% Rh-doped Ru<sub>2</sub>Si<sub>3</sub> prepared by FZ and SPS methods. The SPS method was introduced successfully to produce good thermoelectric materials. The dimensionless thermoelectric figure of merit for 4% Rh-doped Ru<sub>2</sub>Si<sub>3</sub> prepared by FZ+SPS was obtained 0.172 at 1073 K, which reached about 1/3 of optimized Si-Ge.

## References

- 1 D. J. Poutcharovsky and E. Parthé, *Acta Crystallogr. B*, 30 (1974) 2692.
- 2 H. Nowotny, 'The chemistry of extended defects in non-metallic solids', Ed. by L. R. Eyring and M. O'Keefe, North-Holland, Amsterdam 1970, p. 223.
- 3 C. B. Vining, *AIP Conf. Proc.*, 246 (1992) 338.
- 4 C. B. Vining, *Proc. 9<sup>th</sup> Int. Conf. on Thermoelectric Energy Conv.*, 1990, p. 249.
- 5 C. B. Vining and C. E. Allevato, *27<sup>th</sup> Int. Energy Conv. Eng. Conf. Proc.*, 3 (1992) 489.
- 6 T. Ohta, *Proc. 11<sup>th</sup> Int. Conf. on Thermoelectric Energy Conv.*, 1992, p. 74.
- 7 A. Yamamoto, T. Ohta, Y. Sawade, T. Tanaka and K. Kamisato, *Proc. 14<sup>th</sup> Int. Conf. on Thermoelectrics*, 1995, p. 264.
- 8 C. B. Vining and C. E. Allevato, *Proc. 10<sup>th</sup> Int. Conf. on Thermoelectrics*, 1991, p. 167.

- 9 Y. Sawade, T. Ohta, A. Yamamoto, T. Tanaka and K. Kamisato, AIP Conf. Proc., 316 (1994) 99.
- 10 Y. Arita, T. Miyagawa and T. Matsui, Proc. 17<sup>th</sup> Int. Conf. on Thermoelectrics, 1998, p. 394.
- 11 Y. Arita, S. Mitsuda, Y. Nishi, T. Matsui and T. Nagasaki, J. Nucl. Mater., 294 (2001) 202.
- 12 A. Cezairliyan, T. Baba and R. Taylor, Int. J. Thermophysics, 15 (1994) 317.
- 13 J. J. Kuntz, L. Perring, P. Feschotte and J. C. Gachon, J. Solid State Chem., 133 (1997) 439.
- 14 T. Caillat, A. Borshchevsky and J. P. Fleurial, Proc. 12<sup>th</sup> Int. Conf. on Thermoelectrics, 1993, p. 132.
- 15 J. Hesse, Z. Metallkunde, 60 (1969) 652.